Available online at www.sciencedirect.com
ScienceDirect
Electrochimica Acta 52 (2007) 4663–4668
ELECTROCHIMICA Acta
www.elsevier.com/locate/electacta

Synthesis and electrochemical properties of lithium-electroactive surface-stabilized silicon quantum dots

Yoojung Kwon [a], Gyeong-Su Park [b], Jaephil Cho [a,*]

[a] *Department of Applied Chemistry, Kumoh National Institute of Technology, Gumi, Republic of Korea*
[b] *Analytical Engineering Center, Samsung Advanced Institute of Technology, Giheung, Republic of Korea*

Received 9 November 2006; received in revised form 22 January 2007; accepted 27 January 2007
Available online 9 February 2007

Abstract

Highly lithium-electroactive Si quantum dots (*n*-Si), coated with an amorphous carbon layer, were prepared by of butyl-capped Si annealing at 700 or 900 °C. The ordering of the carbon layer structure increased with increasing annealing temperature while the thickness decreased to 1 from 2 nm due to the increased ordering of carbon. *n*-Si, annealed at 900 °C, had the same particle size (5 nm) as *n*-Si annealed at 700 °C. In contrast to Si nanocrystals with an average particle size of 30 nm that had a first charge capacity of 225 mAh/g with a very small coulombic efficiency of 4%, *n*-Si that annealed at 900 °C possessed a first charge capacity of 1257 mAh/g with a significantly enhanced coulombic efficiency of 71%. This improvement was due to the uniform distribution of *n*-Si with a carbon layer that prohibited *n*-Si aggregation during cycling.

Keywords: Si; Nanoparticle; Anode; Li battery; Capacity; Cycle life

1. Introduction

There is presently a large research effort aimed at exploring physical and chemical means to induce a useful level of visible photoluminescence (PL) from silicon quantum dots [1–7]. In this regard, synthesis of Si quantum dots has been intensively studied via controlling the surface chemistry through the attachment of molecular ligands to the surface of the silicon nanocrystals [7–10]. However, the use of this technique has been limited to optical applications. Recently, silicon has shown very large lithium storage capacities and, therefore, is a potential alternative choice among the next generation of high-capacity anode materials in lithium rechargeable batteries. The world-wide market of Li secondary batteries exceeded 5 billion dollars in 2005 and is expected to increase steeply, reaching 10 billion dollars in 2009, as the need for mobile electronics rapidly expands [11]. In this regard, the development of high-capacity lithium anode materials is essential for developing high-capacity lithium secondary batteries. However, while about 3500 mAh/g can be achieved using the first $Li_{4.1}Si$ alloy formation during discharging at room temperature, subsequent lithium dealloying (charging) results in a huge irreversible capacity loss [12–14]. The formation of $Li_{4.1}Si$ alloys induces a 323% volume increase. Such a large volume increase may create microcracks and, therefore, destroy the integrity of the electrode, causing very large irreversible capacity loss and poor cyclability.

There have been many studies to increase the lithium storage ability of Si and improve the cyclability via chemical mixtures of Si particles and carbon precursors, followed by firing or mechanical milling of the mixtures [15–17]. However, these methods did not produce a uniform distribution of Si in the carbon; rather, they resulted in a very irregular distribution of Si particle size. The most effective way to ensure both capacity and cyclability of silicon is to use nanoparticle sizes smaller than 5 nm and to coat the particles with carbon, which acts as a buffer layer during lithium alloying/dealloying. It has been observed that, when the particle size is smaller than 5 nm, particle growth is prohibited, resulting in a retention of the initial particle size [18,19]. However, nanoparticles have a large surface area, which results in severe side reactions with electrolytes, in turn, inducing small coulombic efficiencies (large irreversible capacity) of less then 30%.

At present, alkyl coating is reported to be the most successful colloid technique for growing Si nanocrystals [4], obtained

* Corresponding author. Tel.: +82 54 478 7824; fax: +82 54 478 7710.
E-mail address: jpcho@kumoh.ac.kr (J. Cho).

0013-4686/$ – see front matter © 2007 Elsevier Ltd. All rights reserved.
doi:10.1016/j.electacta.2007.01.077

by the reduction of $SiCl_4$ and $RSiCl_3$ ($R = C_8H_{17}$) in the presence of sodium metal. However, this process should be performed using an organic solvent at 385 °C and high pressure (>1000 atm). Later, the process utilized chlorosilane reduction at room temperature and atmospheric pressure, producing Si nanoclusters of several sizes, and the length of an organic tail was extended [20]. Alkyl capping results from surface passivation with alkyl Li or Grignard reagents and produces particle sizes of smaller than 10 nm. However, but this method is complex. Later, the researchers reported monodisperse silicon nanocrystals (4.5 nm), obtained by reducing $SiCl_4$ with sodium naphthalide at room temperature, using siloxane as a capping agent [21]. Surface ligands with Si–O bonds should not be used due to SiO_x formation during the annealing process. In addition, the nanocrystals should be coated with organic ligands with only C and H, such that they turn into carbon after annealing at high temperatures.

In order to apply this method for anode material production, the yield of final product should be over 40% of the starting $SiCl_4$, and as-prepared *n*-Si should be covered with carbon. We found that a simple modification of Baldwin's methods [22,23] resulted in a high yield and very uniform distribution of *n*-Si with a carbon coating layer. In spite of annealing at 900 °C, uniformly distributed *n*-Si with a uniform carbon coating layer can be obtained.

2. Experimental

Sodium naphthalenide solution was prepared from 1.6 g of sodium and 8 g of naphthalene stirred in 80 ml of 1.2-dimethoxyethane in the glove box. All of the processes were done in the glove box. 2.4 g of $SiCl_4$ and 100 ml of 1,2-dimethoxyethane were thoroughly mixed, followed by pouring into the sodium naphthalide solution and the resulting solution was maintained for 24 h. This mixed solution was stirred for 2 h and then 5 g of butyllithium was added and the resulting solution was stirred for 48 h at 100 rpm at room temperature. When the amounts of sodium and naphthalene were smaller than those described above, the yield rate was less than 10% and particles after annealing were very irregular and severely aggregated (see Fig. 1). A yellow solution was obtained and the solvent and naphthalene were removed by using both a rotating evaporator and a vacuum at 120 °C using excess *n*-hexane. Finally, the resulting orange solution was washed with water six times and heat-treated at 700 and 900 °C for 5 h in a tube furnace under vacuum. Final yield of the *n*-Si was 50% of the starting $SiCl_4$.

The cathodes for the battery test cells were made of *n*-Si, super P carbon black and polyvinylidene fluoride (PVDF) binder (Solef) in a weight ratio of 80:10:10. A loading level of the *n*-Si was 20 mg/cm^2 and its thickness was ~20 μm. The slurry was prepared by thoroughly mixing an *N*-methyl-2-pyrrolidone (NMP) (Aldrich) solution of PVDF, carbon black and the anode material. The coin-type half cells (2016R size), prepared in a helium-filled glove box, contained an *n*-Si, a Li metal, a microporous polyethylene separator and an electrolyte solution of 1 M $LiPF_6$ in ethylene carbonate/dimethyl carbonate (EC/DMC) (1:1 vol.%) (Cheil Industries, Korea).

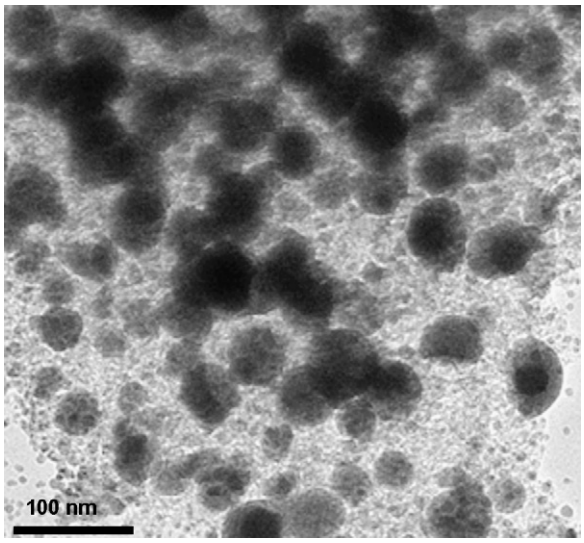

Fig. 1. TEM image of aggregated *n*-Si after annealing at 900 °C.

A field-emission transition electron microscope (FE-TEM) (JEOL 2100F), operating at 200 kV, was used for investigating the microstructure of the samples. Raman spectroscopy (Renishaw 3000) was used to characterize Si nanocrystals confined in the amorphous carbon matrix and to obtain the graphitization degree of the amorphous carbon phase in the sample (ratio of D- and G-band of the carbon) using 633 nm laser excitation. FT-IR spectra (JASCO 4000) for the nanoparticles were obtained at room temperature by dropping the hexane colloid on a KBr plate and allowing the solvent to evaporate. The carbon concentrations in the samples were measured using a CHNS analyzer (Flash EA 1112, Thermo Electron Corp.).

3. Results and discussion

Fig. 2a shows Si nanocrystals, which are commercially available (Nanostructured Materials Inc.). The average particle size is 30 nm and the particles are severely aggregated. Using these nanoparticles as an anode material in a coin-type half cell, electrochemical cycle testing was performed between 1.5 and 0 V with a current of 240 mA/g. Electrochemical property of non-treated Si in Fig. 2 depends on the amounts of the binder and carbon black. In the case of the electrode consisting of active material Si:binder:carbon black with 80:10:10 (wt%), its first discharge and charge capacities 4484 and 225 mAh/g, respectively (Fig. 2b). However, its charge capacity is significantly improved when the electrode consisted of 40:30:30 (wt%), showing 3311 mAh/g. In both cases, the capacity retention after 30 cycles is similar to each other, showing only 5%. The result indicates that non-uniform *n*-Si with aggregation cannot avoid from electrical disconnection of the *n*-Si from the Cu current collector as a result of a greater than 300% volume expansion during repetitive cyclings in spite of increasing amount of carbon black that acts as a buffer layer. This is direct evidence for electrical disconnection of the electrode from the Cu current collector at the edge to the conducting environment in the electrode as a result of a greater than 300% volume expansion of Si.

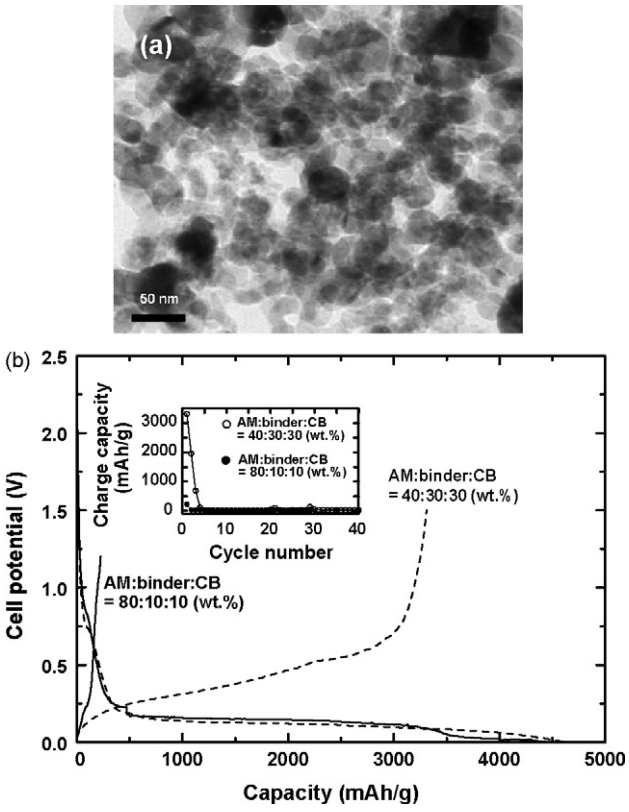

Fig. 2. (a) TEM image of commercially available Si nanopartcles and (b) voltage profiles of the particles with different a weight ratio of Si, binder and carbon black in (a) between 0 and 1.2 V at a rate of 0.2 C. An inserted figure is a plot of the charge capacity vs. cycle number.

Fig. 3 shows FT-IR spectra of the Si nanocrystals capped with butyl groups after annealing at 700 and 900 °C. The peaks at 2964, 2928, 2860, 1461 and 1378 cm^{-1} are assigned to terminal $–CH_3$ asymmetric stretching, $–CH_2$ asymmetric stretching, $–CH_2$ symmetric stretching, terminal $–CH_3$ bending and C–H bending, respectively. Surface oxidation of the Si nanocrystals is very important to reduce the irreversible capacity, and, since butyl-capped *n*-Si before annealing should be washed several times in water and were exposed in air, their surfaces have chances for contamination with oxygen. However, as-prepared samples before and after annealing show no oxide peaks corresponding to Si–O between 1100–1000 and 900–1000 cm^{-1}, indicating no oxygen contamination [20]. However, when the *n*-Si is capped with alkylamine groups, Si–O bonds are formed during annealing process as a result of the decomposition of the alkylamine groups. Due to this reason, we cannot use alkylamine groups as possible capping agents. Note that, after annealing at 700 °C, the peaks assigned to residual butyl groups are observed in the same ranges as before annealing. However, after annealing at 900 °C, peaks assigned to butyl groups completely disappeared and no oxidation peaks are observed.

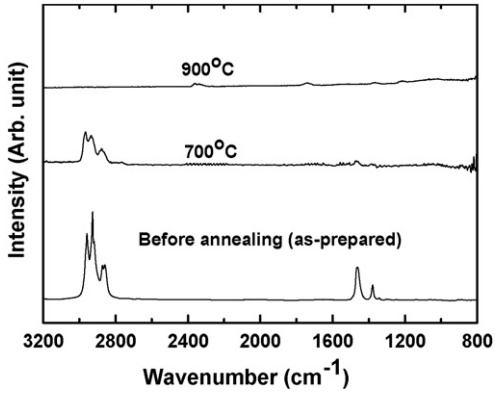

Fig. 3. FT-IR spectra of *n*-Si obtained from annealing at 700 and 900 °C.

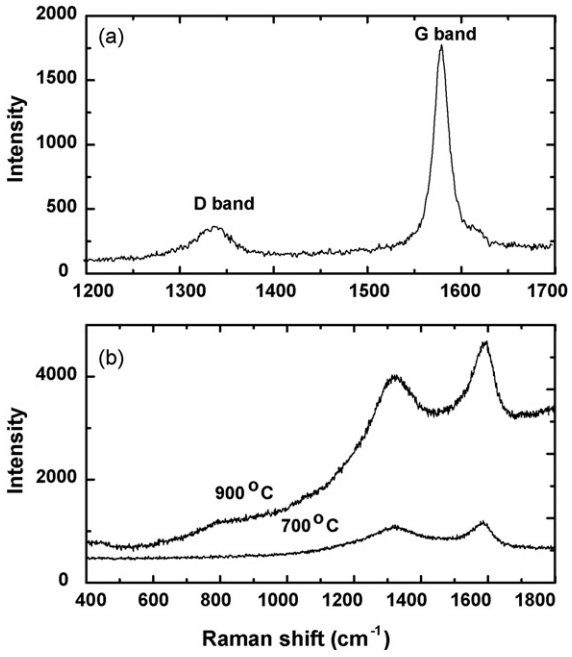

Fig. 4. Raman scattering of (a) fully ordered carbon (synthetic graphite) and (b) *n*-Si obtained from annealing at 700 and 900 °C.

Fig. 4a shows the Raman spectrum of the typically fully ordered carbon, and 1337 and 1579 cm^{-1} peaks are assigned to the D and G bands of carbon, respectively. The ratio of intensities, $I_{D\text{-band}}/I_{G\text{-band}}$, is indicative of the ordering degree of the carbon structure and the value for the fully ordered carbon is estimated to be 0.09. On the other hand, the *n*-Si annealed at 700 and 900 °C resulted in ratios of 2.43 and 1.83, respectively, indicating that both samples have an amorphous nature, and thus Li intercalation/deintercalation may be limited by the carbon layer (Fig. 4b). The sample annealed at 900 °C has a more ordered structure than the sample annealed at 700 °C, and therefore, the sample annealed at 900 °C is expected to show more Li intercalation into the sample. In addition, the lack of a silicon scattering band at 490–520 cm^{-1} supports the TEM result that *n*-Si was fully surrounded by the carbon.

Fig. 5 exhibits the TEM images of butyl-capped Si nanocrystals after annealing at 700 °C (a–c) and 900 °C (d and e). Annealing turned the butyl terminating groups that were electrochemically inactive to electrochemically active amorphous carbon. In the case of the Si nanocrystals annealed at 700 °C, the nanocrystals were monodispersed with a particle size of 5 nm and an expanded image of one *n*-Si clearly shows the lattice fringe of (2 0 0) plane of cubic diamond structure. In addition,

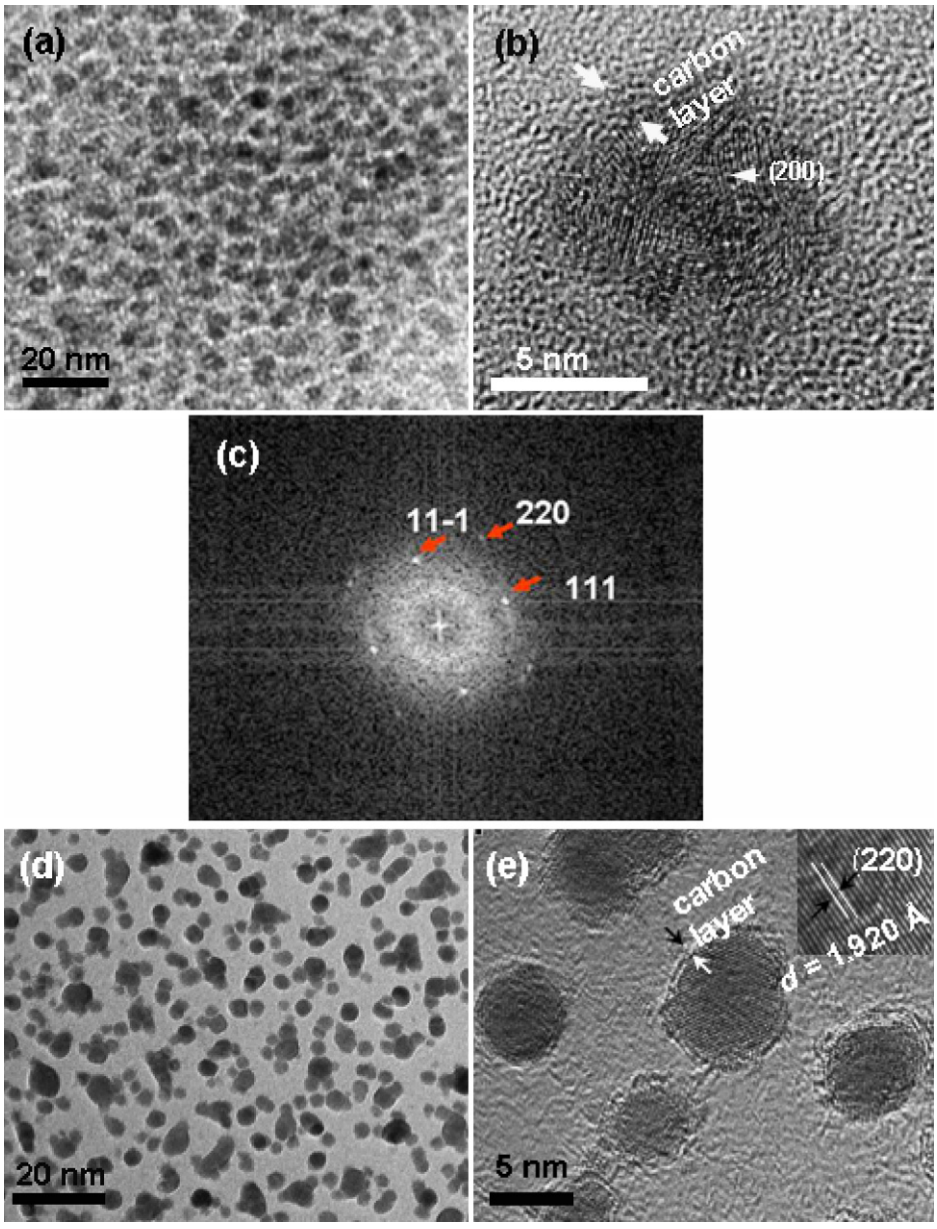

Fig. 5. TEM images of (a) *n*-Si obtained from annealing at 700 °C, (b) expanded image of (a), (c) FFT diffractogram of (a), (d) *n*-Si obtained from annealing at 900 °C and (e) expanded image of (d).

the Fast Fourier Transformed (FFT) diffractogram of Fig. 5c confirms the formation of diamond cubic lattice of silicon. It should also be noted that an amorphous carbon layer with a thickness of ∼2 nm was observed on the particle surface (Fig. 5b). The sample annealed at 900 °C (Fig. 5d and e) shows a similar particle size to that annealed at 700 °C, but the thickness of the carbon layer decreased to ∼1 nm. This indicates that carbon turned into a more ordered structure as evidenced by the Raman scattering.

Fig. 6a shows voltage profiles of the *n*-Si obtained from annealing at 700 and 900 °C between 0 and 1.5 V with a current of 240 mA/g. *n*-Si annealed at 700 °C shows a first discharge and charge capacities of 1644 and 831 mAh/g, respectively, showing a 64% irreversible capacity loss. However, *n*-Si annealed at 900 °C shows much improved charge capacity and decreased irreversible capacity loss with values of 1257 mAh/g and 29%, respectively. The improvement is due to the more ordered carbonaceous structure on the particle surface, which can allow easier lithium intercalation than the hydrophobic alkyl-capping layer. Element analysis confirmed that *n*-Si annealed at 700 °C had 10 wt% carbon and 2 wt% hydrogen. However, that at 900 °C showed no H while maintaining the same amount of carbon content as the sample annealed at 700 °C. This means that residual butyl molecules completely decomposed to an amorphous carbon at 900 °C. Since the contribution from the carbon is estimated to only 10 mAh/g, based upon the charge capacity of amorphous carbon (100 mAh/g) [24], its contribution to the total capacity is negligible. The cycling result of *n*-Si

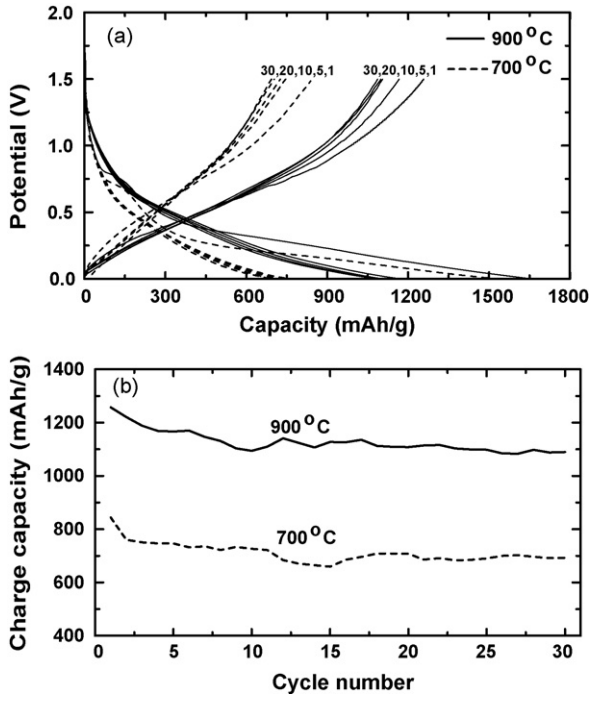

Fig. 6. Plots of (a) voltage profiles of the *n*-Si obtained from annealing at 700 and 900 °C after 1, 5, 10, 20 and 30 cycles between 0 and 1.2 V at a rate of 0.2 C and (b) charge capacity vs. cycle number at a rate of 0.2 C.

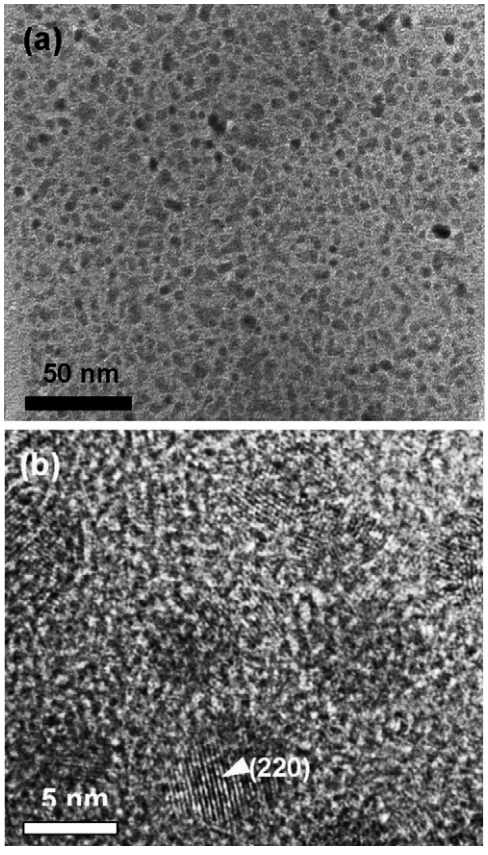

Fig. 7. TEM images of (a) *n*-Si obtained from annealing at 900 °C after cycling and (b) expanded image of (a).

is significantly improved compared with the Si nanocrystals in Fig. 1b. We believe the improvement is associated with two factors: particle size and a carbon layer that acts as a buffer layer for the volume expansion between Si and Li_xSi. In addition, we cannot ignore the contribution of monodispersed *n*-Si and how this reduced particle aggregation that results in rapid particle growth during Li alloying/dealloying. On the other hand, Si nanowires prepared by a laser ablation method demonstrated a reversible capacity of ~600 mAh/g only [14].

Capacity retention results in Fig. 6b shows better capacity retention of the sample annealed at 900 °C than that at 700 °C, showing 84% after 30 cycles. This shows direct evidence that the factor described above affects the ability of the electrode to retain its integrity during cycling. In addition, considering that Si nanoparticles have larger than a 80% irreversible capacity loss, our sample shows significant improvement. Fig. 7 exhibits the TEM images of the samples annealed at 700 °C after cycling giving direct evidence for the change in particle size. Particle growth of the lithium active metals is common phenomena even though its growth depends on the original particle size and uniformity. Fig. 7 (TEM image) shows evidence that the cycled sample shows no particle growth after cycling, retaining its initial particle size of 5 nm. In nanomaterials, the energy barriers for alloy formation are smaller than in bulk materials because a large fraction of the Si atoms are in high energy states on the highly curvatured surfaces. In this regard, the large volume change due to nucleation of the new phase (Li_xSi) can be readily accommodated [14].

4. Conclusion

Annealed *n*-Si, capped with a carbon layer, exhibited significantly improved capacity and capacity retention, as compared to conventional Si nanoparticles. In particular, *n*-Si, annealed at 900 °C, showed uniformly dispersed particles with a carbon layer thickness of 1 nm and did not show any SiO_x contamination. These particles showed a first charge capacity of 1257 mAh/g, with an irreversible capacity loss of 29%. Furthermore, capacity retention after 30 cycles was 84%. Even so, we need to improve the yield up to 70% of the preparation of the *n*-Si in order to make this reduction method competitive with other ball milling methods.

Acknowledgement

This work was supported by grant No. B1220-0501-0019 from the University Fundamental Research Program of the Ministry of Information & Communication in Republic of Korea

References

[1] J.H. Warner, A. Hoshino, K. Yamamoto, R.D. Tilley, Angew. Chem. Int. Ed. 44 (2005) 4550.
[2] J.D. Holmes, K.J. Ziegler, R.C. Doty, L.E. Pell, K.P. Johnston, B. Krogel, J. Am. Chem. Soc. 123 (2001) 3743.
[3] W.L. Wilson, P.F. Szajowski, L.E. Brus, Science 262 (1993) 1242;
K. Littau, P.J. Szajowski, A.J. Muller, A.R. Kortan, L.E. Brus, J. Phys. Chem. 97 (1993) 1224;

L.E. Brus, P.F. Szajowski, W.L. Wilson, T.D. Harris, S. Schuppler, P.H. Citrin, J. Am. Chem. Soc. 117 (1995) 2915;
L. Brus, J. Phys. Chem. 98 (1994) 3575.
[4] J.R. Heath, Science 258 (1992) 1131;
P.E. Batson, J.R. Heath, Phys. Rev. Lett. 71 (1993) 911.
[5] C.-S. Yang, R.A. Bley, S.M. Kauzlarich, H.W. Lee, G.R. Delgado, J. Am. Chem. Soc. 121 (1999) 5191.
[6] (a) J.P. Wilcoxon, G.A. Samara, Appl. Phys. Lett. 74 (1999) 3164;
(b) J.P. Wilcoxon, G.A. Samara, P.N. Provencio, Phys. Rev. B 60 (1999) 2704.
[7] R.A. Bley, S.M. Kauzlarich, J. Am. Chem. Soc. 118 (1996) 12461.
[8] O. Akcakir, J. Therrien, G. Belomoin, N. Barry, E. Gratton, M. Nayfeh, Appl. Phys. Lett. 76 (2000) 1857.
[9] A.B. Sieval, A.L. Demirel, J.W.M. Nissink, M.R. Linford, J.H. van der Maas, W.H. De Jeu, H. Zuilhof, E.J.R. Sudholter, Langmuir 14 (1998) 1759.
[10] J. Ji, Y. Chen, R.A. Senter, J.L. Coffer, Chem. Mater. 13 (2001) 4783.
[11] Annual Report on Advanced Rechargeable Battery Industry in 2005, Nomura Research Institute Ltd., Japan, 2006.
[12] M.N. Obrovac, L. Christensen, Electrochem. Solid State Lett. 7 (2004) A93.
[13] N. Dimov, S. Kugino, M. Yoshio, J. Power Sources 136 (2004) 108.
[14] B. Gao, S. Sinha, L. Fleming, O. Zhou, Adv. Mater. 13 (2001) 816.
[15] I.-S. Kim, G.E. Blomgren, P.N. Kumta, Electrochem. Solid State Lett. 7 (2004) A44.
[16] G.X. Wang, J. Yao, H.K. Liu, Electrochem. Solid State Lett. 7 (2004) A250.
[17] J. Yang, B.F. Wang, K. Wang, Y. Liu, J.Y. Xie, Z.S. Wen, Electrochem. Solid State Lett. 6 (2003) A154.
[18] E. Kim, M.G. Kim, J. Cho, Electrochem. Solid State Lett. 9 (2006) 311.
[19] C. Kim, M. Noh, M. Choi, J. Cho, B. Park, Chem. Mater. 17 (2005) 3297.
[20] C.-S. Yang, R.A. Bley, S.M. Kauzlarich, H.W.H. Lee, G.R. Delgado, J. Am. Chem. Soc. 121 (1999) 5191.
[21] J. Zou, K. Baldwin, A. Katherine, A. Pettigrew, S.M. Kauzlarich, Nano Lett. 4 (2004) 1181.
[22] R.K. Baldwin, K.A. Pettigrew, E. Ratai, M.P. Augustine, S.M. Kauzlarich, Chem. Commun. (2002) 1822.
[23] R.K. Baldwin, K.A. Pettigrew, J.C. Garno, P.P. Power, G. Liu, S.M. Kauzlarich, J. Am. Chem. Soc. 124 (2002) 1150.
[24] M. Noh, H. Lee, Y. Kwon, J. Cho, Y. Kim, M.G. Kim, Chem. Mater. 17 (2005) 1926.